Aggregation–Disaggregation Cycles in ERA5 Reanalysis

VIJIT MAITHEL[a,b] AND LARISSA BACK[b]

[a] *CIRES, University of Colorado Boulder, Boulder, Colorado*
[b] *University of Wisconsin–Madison, Madison, Wisconsin*

(Manuscript received 15 December 2023, in final form 31 August 2024, accepted 26 September 2024)

ABSTRACT: Understanding convective aggregation is very important for understanding tropical climate and climate sensitivity. However, we still lack a full understanding of how aggregation evolves in the real world or what phenomena and scales are analogous to the self-aggregation observed in idealized models. In this study, we apply the moist static energy (MSE) variance budget framework to ERA5 reanalysis data to study the evolution of large-scale aggregation over tropical oceans at basinwide scales. Our novel phase space diagnostics focus on the variability of observed aggregation compared to most previous self-aggregation studies, which focus more on the aggregated mean state. We visualize observed aggregation to evolve anomalously around a mean state in a cyclical fashion forming aggregation–disaggregation cycles. We find horizontal advection of MSE to play the primary role in determining when the domain aggregates or disaggregates. In contrast, all advective, radiative, and surface flux feedbacks are found important for determining the magnitude of the aggregation anomalies. Surface fluxes and horizontal advection tend to dampen aggregation anomalies, while radiative fluxes and vertical advection tend to amplify aggregation anomalies. Looking deeper into the advection terms, we find that changes in vertical advection are dominated by enhanced low-level subsidence over the dry regions during the more aggregated states. This creates an anomalous drying tendency over the dry regions, which maintains aggregation anomalies. In contrast, horizontal advection changes are found to be dominated by increased moisture advection out of the moist columns with stronger aggregation.

SIGNIFICANCE STATEMENT: The purpose of this study is to characterize and understand the evolution of large-scale convective aggregation in the real world through reanalysis data. While most previous observational studies have focused on the evolution of clouds and cloud populations with aggregation, we focus on the energetics and the impact of aggregation on redistributing moisture throughout the domain. Our framework highlights that aggregation can be visualized as a continuously occurring cyclic feature at large scales in the tropics. Further, our work provides a deeper insight into the changes in large-scale circulation that accompany aggregation and characterizes the similarities and differences between the different regions in the tropics.

KEYWORDS: Advection; Cloud radiative effects; Energy budget/balance; Reanalysis data; Tropical variability

1. Introduction

Convective aggregation is generally used to refer to the clustering of clouds (and hence convection) in a nonrandom manner in a domain. It arises as a result of feedbacks between convection, circulation, moisture, and radiation under uniform or nonuniform boundary conditions. Idealized numerical models have been extensively used to study the characteristics of convective aggregation under uniform boundary conditions, also referred to as convective self-aggregation (Bretherton et al. 2005; Held et al. 1993) since external forcings are constant in space and time. In contrast, convection in the real world does experience nonuniform boundary conditions which can vary in both space and time. This impacts how convection aggregates in the real world and is termed as convective aggregation to differentiate it from self-aggregation. It is not completely clear what role or relevance the mechanisms behind self-aggregation play when it comes to aggregation in the real world [review by Holloway et al. (2017)]. However, there are some key characteristics that have been identified in how both self-aggregation and aggregation can impact the spatial domain. Studies have shown that the domain consistently becomes drier, outgoing longwave radiation (OLR) increases, and spatial gradients of column water vapor in the domain increase as it becomes more aggregated, in both idealized models (Bretherton et al. 2005; Wing and Emanuel 2014; Wing and Cronin 2016; Holloway and Woolnough 2016, etc.) and observations (Tobin et al. 2012; Tsai and Mapes 2022; Stein et al. 2017; Bony et al. 2020, etc.). This robust impact of aggregation on the large-scale environment, combined with the dependence of aggregation on sea surface temperatures (SSTs) (Cronin and Wing 2017; Coppin and Bony 2015), makes understanding convective aggregation extremely important to understanding climate sensitivity [review by Wing (2019) and Becker and Wing (2020)].

To understand links between aggregation and self-aggregation, we first need to understand the nature of convective aggregation in the real world and what aspects may connect to the model world. Generally, convection in such idealized modeling studies is in radiative–convective equilibrium (RCE) and starts off from an equilibrium state with convection randomly distributed across the domain. Then, with time, the domain slowly transitions to a new equilibrium state, still in RCE but with clustered or aggregated convection. On attaining self-aggregation, the model will

Corresponding author: Vijit Maithel, vijit.maithel@noaa.gov

DOI: 10.1175/JCLI-D-23-0750.1

typically maintain itself in that state. In contrast, in the real world, convection is already in an aggregated state due to the presence of external boundary conditions and feedbacks from previous convective events. However, the extent of aggregation can change with time. This will result in a mean aggregated state of the domain and phases when the domain is aggregating or disaggregating with respect to the mean state. In this regard, the factors in the idealized simulations that maintain the aggregated equilibrium state and the factors that control the variability of aggregation in models around the mean state are most relevant for the real world. Patrizio and Randall (2019) highlight a slow oscillation observed in their model runs once the domain self-aggregates. Similar oscillations can also be observed in some other modeling studies (Silvers et al. 2016; Arnold and Randall 2015). However, previous studies have mainly focused on the maintenance of the mean state, while the variability has not been studied systematically. This study presents a framework that characterizes the feedback processes associated with the variability of aggregation. The results highlight the cyclic nature of the variability which we term as aggregation–disaggregation cycles. While this framework is applied to look at aggregation in real-world conditions in this study, applications to idealized modeling studies are left for future work.

To measure the extent of aggregation in observations, previous studies have used a variety of cloud-clustering-based metrics. Each of these metrics, in some way or the other, combines different cloud properties from satellite observations to quantify cloud clusters so as to act as an aggregation metric. Some prominent metrics in use are the simple convective aggregation index (SCAI; Tobin et al. 2012), the organization index I_{org} (Tompkins and Semie 2017), the morphological index of convective aggregation (MICA; Kadoya and Masunaga 2018), etc. However, there can be some concerns about how well these metrics correlate with larger-scale convective organization. For example, Sakaeda and Torri (2022) show that self-aggregation-based cloud metrics do not necessarily correlate well with the Madden–Julian oscillation (MJO) phase index. They show that many metrics are unable to show an increase in aggregation during the active MJO phase, and some even show that convection becomes less aggregated during the MJO active phase. They highlight that these discrepancies primarily arise because of how these metrics can be biased toward particular cloud properties by construction (like cloud clusters becoming larger or clusters becoming fewer) and individually may not fully capture all characteristics of cloud evolution.

Such factors make it difficult to quantify aggregation in a way that facilitates easier comparison between self-aggregation in idealized models with aggregation in the real world. However, since aggregation in both models and observations has shown consistent and strong impacts on the large-scale environment (Wing 2019), there is potential to define aggregation based on the state of the large-scale environment itself. A particularly strong, robust, and easy-to-track metric for doing so is the spatial variability of column water vapor. Motivation for using this metric is twofold. First, the column water vapor distribution has been shown to vary with aggregation significantly in both observations (Lebsock et al. 2017; Tsai and Mapes 2022; Beucler et al. 2020) and models (Bretherton et al. 2005; Wing and Emanuel 2014; Beucler et al. 2020). Second, empirical evidence shows a strong dependence of precipitation on a critical moisture threshold (Bretherton et al. 2004) and the existence of sharp water vapor margins for the intertropical convergence zones (ITCZs) (Mapes et al. 2018; Beucler et al. 2020). This suggests that convection, aggregation, and the distribution of column moisture in the tropics are strongly interconnected with each other. Aggregation can impact the distribution of water vapor in the tropics and vice versa.

Previous studies have successfully used this to define new metrics for aggregation and use them to compare self-aggregation in idealized models and aggregation in the real world. Lebsock et al. (2017) verified that the spatial variance of column water vapor can be used as a metric for aggregation using satellite data. Beucler et al. (2020) define a metric for aggregation based on the length of the margin surrounding the moist region. Beucler et al. (2019, 2020) provide a process-level comparison between aggregation in reanalysis data and idealized models.

This also provides strong support to the idea that self-aggregation mechanisms can be relevant for understanding convective variability that is driven by changes in moisture in the real world (Adames Corraliza and Mayta 2024; Tsai and Mapes 2022). Other recent studies have highlighted such moisture-driven modes of convective variability being observed ubiquitously throughout the tropics (Inoue and Back 2017) and the mechanisms behind them to be inherent to how convection interacts with the large-scale environment (Inoue et al. 2021; Maithel and Back 2022).

Altogether, this suggests that studying the evolution of moisture and its variance is a way of tracking aggregation. Owing to the weak temperature gradient (WTG) approximation (Sobel et al. 2001), the evolution of moisture can be studied using moist static energy (MSE) budgets, and the variance of moisture can be studied using the MSE variance budget. While the MSE budget [Eq. (1)] has been extensively used to study moisture-driven convective variability, the MSE variance budget [Eq. (2)] (Wing and Emanuel 2014) has been extensively used to study self-aggregation and for tropical cyclone diagnostics (Wing and Emanuel 2014; Coppin and Bony 2015; Holloway and Woolnough 2016; Wing et al. 2019; Dirkes et al. 2023, etc.):

$$\frac{\partial \langle h \rangle}{\partial t} = \mathrm{VADV} + \mathrm{HADV} + \langle Q_R \rangle + \mathrm{SF} + \mathrm{Res}, \tag{1}$$

$$\begin{aligned} \frac{1}{2}\frac{\partial \langle h \rangle'^2}{\partial t} = {} & \langle h \rangle' \mathrm{VADV}' + \langle h \rangle' \mathrm{HADV}' + \langle h \rangle' \langle \mathrm{Q_R} \rangle' \\ & + \langle h \rangle' \mathrm{SF}' + \langle h \rangle' \mathrm{Res}' \\ \mathrm{VADV} = {} & -\langle \omega \partial h / \partial p \rangle \\ \mathrm{HADV} = {} & -\langle \mathbf{v} \cdot \nabla h \rangle. \end{aligned} \tag{2}$$

In Eqs. (1) and (2), $\langle \dots \rangle$ represents the mass-weighted vertical column integral from the surface to 100 hPa, $'$ represents the anomaly compared to the domain mean, h represents the MSE, ω represents the vertical velocity in pressure coordinates, $\mathbf{v}$ is the horizontal wind vector, VADV and HADV stand for the vertical advection and the horizontal advection, respectively, $\langle Q_R \rangle$ is the column radiative flux, SF is the

surface sensible and latent heat flux, and Res stands for the residual term. Most idealized modeling studies, which have used MSE variance budget to study aggregation, generally define the advection terms together as a single term calculated as a budget residual (Wing and Emanuel 2014; Holloway and Woolnough 2016; Pope et al. 2021, etc.), or they compute the advection term explicitly but do not break it down between vertical and horizontal advection components (Wing 2022). However, this decomposition has been extensively used in the literature to understand the evolution of MSE budgets (Back and Bretherton 2006; Maloney 2009; Adames and Maloney 2021, etc.). Therefore, we choose to break down the advection term into two components and keep a separate residual term to close the budget.

The MSE variance budget framework (Wing and Emanuel 2014) makes use of the observation that self-aggregation results in the redistribution of moisture and MSE within the domain to resemble a bimodal distribution with anomalously moist and dry columns instead of being more uniformly distributed (Bretherton et al. 2005). This implies an increase in the value of the spatial variance of MSE with aggregation. Furthermore, the MSE variance budget [Eq. (2)] can be used to measure how different processes contribute to the increase or decrease in MSE variance. It is derived by multiplying the spatial anomalies of the terms in Eq. (1) with the spatially anomalous column MSE at each time instant. A positive variance budget term represents that the anomalously moist columns in the domain tend to further moisten as a result of that process or anomalously dry columns will tend to further dry up. This implies that the term tends to act as a positive feedback on column MSE anomalies. Since amplifying or sustaining existing MSE anomalies helps aggregation, positive feedbacks on MSE anomalies support aggregation. Consequently, a negative variance budget term signifies that the term acts as a negative feedback on column MSE anomalies and does not support aggregation.

Using the MSE variance budget, idealized modeling studies found the positive feedback of radiative fluxes on column MSE anomalies to be the dominant mechanism responsible for initiation as well as maintenance of the self-aggregated mean state (Wing et al. 2017; Pope et al. 2021, 2023; Beucler et al. 2019). This is supported by observations which showed that at large scales, anomalous column radiative fluxes vary linearly with anomalous column moisture with a positive regression coefficient (Su and Neelin 2002; Inoue and Back 2017). This implies that positive moisture anomalies are linked with anomalous moistening tendency or negative moisture anomalies are linked with anomalous drying tendency, that is, radiative fluxes act as a positive feedback on MSE anomalies. Moreover, the positive coefficient also implies that the feedback is expected to get stronger with larger anomalies. However, this only shows that radiative anomalies strongly covary with MSE or moisture anomalies. This does not tell us about the causality. In other words, are changes in MSE anomalies or changes in aggregation driven by changes in radiative feedbacks? Many recent studies looking at the evolution of the aforementioned moisture-driven convective variability modes in observations have found the tendencies in column MSE to be driven strongly by advection instead of radiation, with radiation being important for maintenance (Inoue et al. 2021; Maithel and Back 2022; Mayta and Adames Corraliza 2024).

This is the main question investigated in this study. What drives the variability of aggregation in the real world? Does convection aggregate/disaggregate following the strengthening/weakening of the positive feedback from radiative fluxes? Or do radiative feedbacks contribute to determining the extent of aggregation whereas advective processes determine when it aggregates and disaggregates? We hypothesize that advection of MSE plays a large role in driving aggregation–disaggregation cycles in observations and our hypothesis is supported by the analysis in this paper. We use the spatial variance of MSE as our metric of aggregation.

The rest of this paper is structured as follows. Section 2 describes the dataset being used and how the variance budget calculation is set up. It also introduces the novel variance phase space that we will use as our diagnostic framework. Section 3 presents the main results from the study, while section 4 presents the summary and discussion.

2. Data and methods

For this study, we use ERA5 data as our observationally constrained view of the real world. Temperature, humidity, winds, radiation, and sensible and latent heat surface fluxes are used from ERA5 to compute the column-integrated MSE and column-integrated MSE budget time series at each grid point. Column-integrated quantities are computed by taking the vertical integral across 27 vertical levels between 1000 and 100 hPa. Further, the MSE variance budget terms are computed over four large domain boxes, each corresponding to the four main tropical ocean basins: an Indian Ocean (IO) box spanning between 10°S–5°N and 55°–95°E, a western Pacific (WP) box spanning between 5°S–10°N and 150°E–180°, an eastern Pacific (EP) box spanning between 0°–15°N and 195°–265°E, and an Atlantic Ocean (AO) box spanning between 0°–15°N and 315°–340°E. We use data at a horizontal resolution of 0.5° × 0.5° and a time resolution of 6 h from 1980 to 2019 within each box. The MSE budget time series at each grid point is further passed through a 24-h running mean filter to remove diurnal variability from the data.

The domains we use are much larger than the 10° × 10° or 5° × 5° boxes used to evaluate the cloud-based aggregation metrics in previous studies. In this study, we are focusing on defining aggregation through its impact on the large-scale distribution of MSE, hence the need for a larger domain size to sample both the moist and dry regions. Because of the larger domain size, the domains can be expected to be closer to radiative–convective equilibrium (RCE) more frequently (Jakob et al. 2019). Larger domains also put more emphasis on convective features and aggregation at larger spatiotemporal scales (like the ITCZ) which evolve more slowly at subseasonal time scales. It should be noted that the majority of the existing literature on convective aggregation in observations is instead focused more at cloud organization at mesoscales.

The MSE variance budget terms are calculated as follows from the MSE budget. First, for each grid point, the spatial

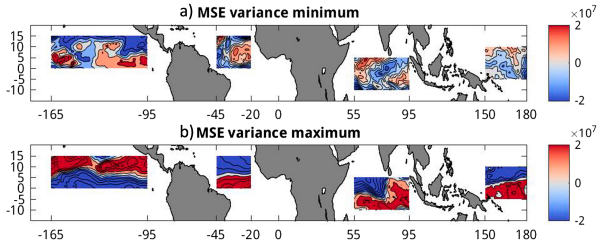

FIG. 1. Snapshots showing the spatial structure of the column MSE anomalies (J m^{-2}) in the four ocean basin domains being studied when (a) each domain has minimum MSE variance and (b) each domain has maximum MSE variance. Both (a) and (b) follow the same color bar.

anomaly of column MSE and each of the budget terms is computed by subtracting the respective domain mean at each time step. Then, the MSE budget term anomaly is multiplied with the column MSE anomaly at each grid point. Finally, a domain mean of the product of the anomalies is calculated. This gives a one-dimensional time series to represent each term in Eq. (1) in each of the four ocean boxes. In the rest of this paper, it is implied that any reference to MSE variance or MSE variance budget term means reference to the domain mean quantity unless otherwise specified. Figure 1 shows a snapshot of the spatial distribution of column MSE anomalies when the MSE variance is minimum (top) and when the MSE variance is maximum (bottom) for each of the four boxes. As expected, high MSE variance snapshots look more aggregated. A strongly aggregated domain in this framework looks like a strong latitudinal ITCZ band with sharp margins and a larger MSE gradient.

We propose to use a novel MSE variance-based phase space to visualize the variability and evolution of MSE variance. The phase space is formed by taking the MSE variance on the x axis and the MSE variance tendency on the y axis. While the x axis physically corresponds to the extent or degree of aggregation in the domain, the y axis represents the process: whether it is undergoing aggregation (increasing variance) or disaggregation (decreasing variance). A schematic of an idealized aggregation–disaggregation cycle is shown in Fig. 2a. The arrows depict the expected trajectory on the phase space as MSE variance changes. When the domain aggregates, MSE variance will increase related to positive variance tendency (arrow going left to right), and when it disaggregates, MSE variance will decrease related to negative variance tendency (arrow going right to left).

The main idea is that the phase space allows us to visualize the different phases of this cycle and look at how the contributions from the various terms in Eq. (2) change across the different phases. More and less aggregated phases are the right and left halves, respectively, and aggregating and disaggregating phases are the top and bottom halves, respectively.

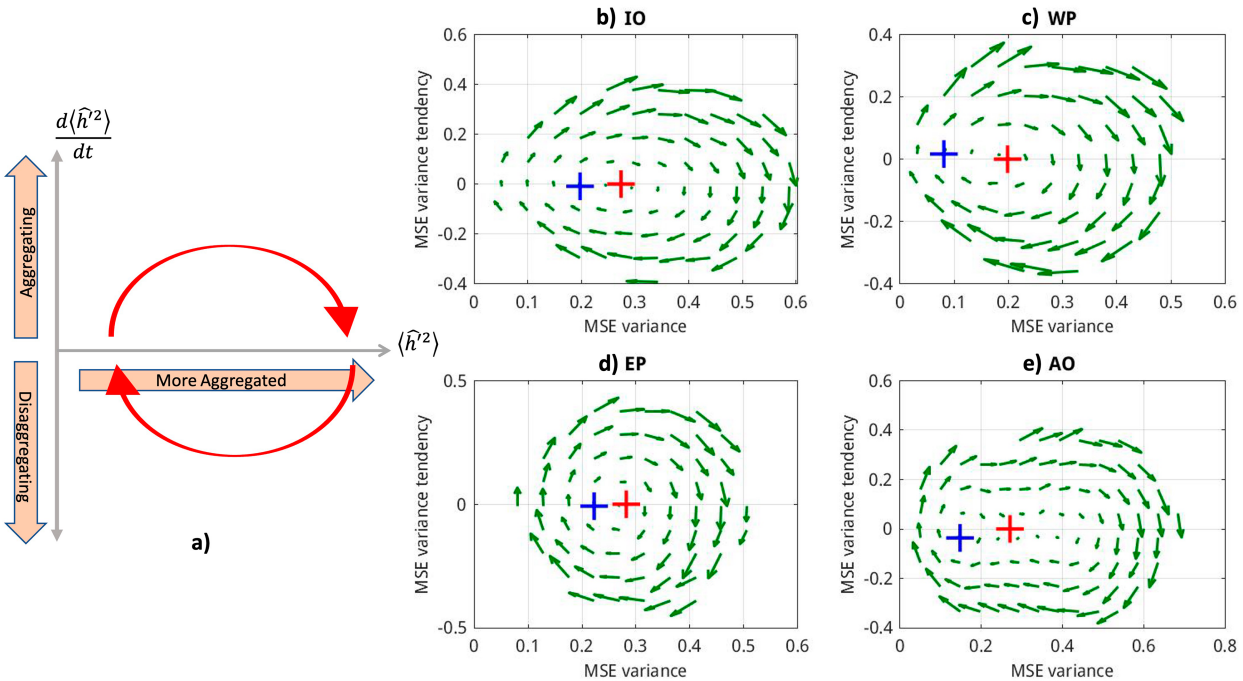

FIG. 2. (a) A simple schematic of the MSE variance phase space and the idealized aggregation–disaggregation cycle. The x axis is the domain mean MSE variance, and the y axis is the tendency of domain mean MSE variance. Both the axes have been normalized and are dimensionless. Red arrows represent what a typical aggregation–disaggregation cycle would look like. Vector plot showing the actual evolution on the MSE variance phase plane in reanalysis data for the four ocean basins (b) IO, (c) WP, (d) EP, and (e) AO. For easier visualization, the phase plane has been divided into 400 equally spaced bins (20 along each axis) and bin mean values have been plotted. Only bins with more than 100 samples are shown. The red and blue markers denote the mean and mode of the distribution, respectively.

This picture emphasizes the transient part of large-scale aggregation in the observed world, which is continuously varying and evolving.

We also choose to normalize the MSE variance and MSE variance budget terms so that the two-phase plane axes have similar magnitudes for better visualization. We do so by dividing the MSE variance time series for each domain by the maximum MSE variance observed in that domain and the MSE variance tendency by the maximum absolute value of the MSE variance tendency in the domain. As a result, the x axis on the phase plane has a range between 0 and 1, and the y axis has a range between -1 and 1. Other MSE variance budget terms from Eq. (2) are normalized by the same maximum MSE variance tendency value.

3. Results

We will start with looking at the representation of the mean aggregated state and the variability in aggregation about the mean state on the phase space. We characterize the evolution of the variability in aggregation by plotting a phase portrait. The phase portrait shows the vectors corresponding to the expected direction of evolution on the phase plane given the current state/location on the phase space. The vectors are computed by first computing the time derivatives of MSE variance and MSE variance tendency at each time step. Then, the phase plane is divided into 400 small rectangular bins (20 equally spaced bins along each axis). Then, we compute the bin mean time derivative of the MSE variance (vector magnitude along the x axis) and the bin mean time derivative of the MSE variance tendency (vector magnitude along the y axis) for each bin. The resulting bin mean vectors for each ocean basin are plotted in Figs. 2b–e. Only bins with more than 100 samples are plotted. We observe that aggregation in ERA5 tends to evolve in a cyclic fashion as visualized in the simple schematic in Fig. 2a for aggregation–disaggregation cycles. This is observed universally in the different ocean basin boxes. Additionally, the red and blue markers correspond to the mean and the mode of the binned two-dimensional distribution. This signifies that the aggregation–disaggregation cycles are a mode of variability about the mean state representing how the system tends to evolve when it is perturbed from its mean and/or most frequent state.

It should be noted that since we have not used any time filtering apart from the 24-h running mean filter, the phase portraits in Fig. 2 are a mix of different time scales including the seasonal cycle and interannual modes. Slow modes of variability like the seasonal cycle, monsoons, and El Niño–Southern Oscillation (ENSO) are associated with the slow-evolving shorter vectors on the phase portrait, and the larger vectors are associated with higher frequency variability at subseasonal time scales. Based on a power spectrum analysis, we expect the aggregation–disaggregation cycles to be associated with 10–60-day time scale (not shown). While a more careful and comprehensive analysis of the variability at different time scales is out of scope for this work, that is an important direction for future work.

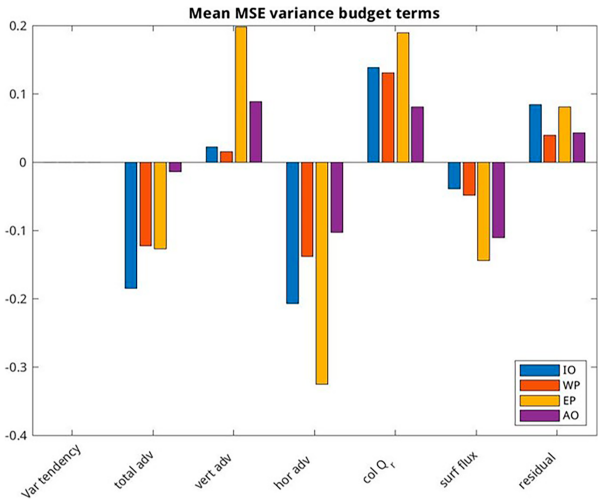

FIG. 3. Bar plot showing the mean MSE variance budget terms from Eq. (2) over the full time series. A residual term is also computed to accommodate the fact that the MSE budget is not exactly closed in ERA5 data. Different colors correspond to different ocean basins with IO in blue, WP in orange, EP in yellow, and AO in purple. The MSE variance budget terms are unitless because of normalization.

a. *Contributions to the mean aggregated state*

Before we delve deeper into looking at this cyclic behavior, we characterize the mean state of aggregation in reanalysis by plotting the mean value of the MSE variance budget terms over the full time series. Figure 3 shows the mean MSE variance budget terms for each ocean basin. Since the mean MSE variance tendency is zero in this figure, these values can be compared qualitatively with those during the equilibrium part of the idealized model simulations when the domain has already reached an aggregated equilibrium state.

From Fig. 3, we observe that the column radiative and surface fluxes act as mean positive and negative feedbacks on column MSE anomalies, respectively, in all ocean basins. Hence, mean radiative fluxes support aggregation and mean surface fluxes resist aggregation. This is consistent with the results in Beucler et al. (2019) for reanalysis and satellite data. This is also broadly consistent with the results in Pope et al. (2023) who thoroughly analyzed the diabatic flux feedbacks in the different models run as part of the Radiative–Convective Equilibrium Model Intercomparison Project (RCEMIP; Wing et al. 2018, 2020). Pope et al. (2023) found the trapping of outgoing longwave radiation by high clouds and absorption of shortwave radiation by water vapor in the moist regions as the dominant mechanisms that help explain the positive radiative feedback. Regarding surface flux feedbacks, we observe that in ERA5 they tend to resist aggregation during all phases of the cycle in all ocean basins. A possible hypothesis for this could be that surface fluxes are dominated by negative feedback processes which tend to moisten dry regions compared to positive feedback processes like the wind-driven surface heat exchange (WISHE) feedback which will tend to moisten the

moist regions. Such negative feedback processes in dry regions could be related to increased air–sea enthalpy disequilibrium (Wing and Emanuel 2014) and are consistent with Bretherton and Khairoutdinov (2015) that found anomalous surface fluxes dominated by increases in dry intrusions.

Vertical advection displays large qualitative differences between the different basins. While over the eastern Pacific and Atlantic Ocean basins, vertical advection has a strong mean positive feedback on MSE anomalies, over the Indian Ocean and western Pacific basins, the mean feedback is closer to zero and smaller than the residual. This is interesting because this is the opposite of what would be expected from a traditional Hadley cell picture for the mean tropical circulation. Based on the Hadley cell, one will expect net energy transport from tropics toward subtropics. This can be associated with energy export by the upper-level branch of the Hadley cell through a negative vertical MSE advection over the ascending columns. Since energy is expected to be transported from moist to dry columns, this should lead to a negative vertical advection feedback term here. Instead, Fig. 3 suggests that the mean overturning circulation does not transfer MSE effectively from moist to dry regions at these scales and can even transport MSE upgradient. Contribution from horizontal advection of MSE is important for understanding the net advection term. A possible explanation for the interbasin differences in vertical advection feedback could be related to differences in vertical motion profile shape. Back and Bretherton (2006) and Back et al. (2017) showed that climatological vertical motion profile shapes being more bottom heavy in the eastern Pacific and Atlantic Ocean can lead to negative gross moist stability values in the region.

Further, we observe that horizontal advection acts as a mean negative feedback on MSE anomalies in all ocean basins. This motivates thinking of horizontal advection as a mixing term which physically tends to reduce MSE gradients in the domain. It is interesting to note that total advection acts as an overall negative feedback on MSE anomalies (with the exception of the Atlantic basin) suggesting that horizontal advection feedbacks dominate vertical advection feedbacks. While most models do not compute the vertical and horizontal advection variance terms explicitly to compare with reanalysis here, Pope et al. (2023) do find total advection to act as a net negative feedback in RCEMIP model runs once the models have reached an aggregated state. The net variance from advection is also negative in the results presented in Beucler et al. (2019) for ERA5 data.

b. *Contributions to the variability about the mean state–qualitative assessment*

As shown in Fig. 2, a robust cyclic variability is observed about the mean aggregated state. Physically, this implies that day-to-day variability in aggregation exhibits deviations from the mean state which evolve in a cyclic fashion around the mean state. We are interested in understanding what drives this cyclic behavior in aggregation. There can be two aspects to this: first, what determines when the domain aggregates or disaggregates, and second, what determines how much the domain aggregates or disaggregates.

One way to do so is to understand the contribution of each of the MSE variance budget terms in Eq. (2) to the variability in MSE variance and the variability in MSE variance tendency. While MSE variance is a metric of how much the domain is aggregated, MSE variance tendency is an indicator of when the domain aggregates or disaggregates. Figure 4 shows the bin mean values of the MSE variance budget terms across different phases on the phase space in the different ocean basins. The change in budget term values along the x and y directions on the phase space tells us about how the term covaries with and contributes to variability in MSE variance and MSE variance tendency, respectively.

Overall, we observe important patterns that are consistent across the different ocean basins. These are discussed below. There are also some differences between the different ocean basins which will be discussed more in subsequent subsections.

Variance from horizontal advection is the only term which varies in magnitude along the y direction (Figs. 4e–h). Horizontal advection variance increases in magnitude as the MSE variance tendency increases. The three remaining terms, variance from vertical advection, radiative fluxes, and surface fluxes, vary primarily along the x direction. This implies that only horizontal advection variance positively covaries with MSE variance tendency; that is, only the value of horizontal advection variance changes with changes in MSE variance tendency for a given value of aggregation. Therefore, horizontal advection variance is of first-order importance for determining changes in MSE variance tendency and hence when the domain aggregates or disaggregates. On the other hand, all four terms show variability along the x direction. This indicates that all four terms play a role in determining variability in MSE variance and therefore how much the domain aggregates.

This ties back in with our initial hypothesis that diabatic terms may not necessarily be the driving force behind the observed aggregation–disaggregation cycles. Horizontal advection seems to be the key factor for determining when things will aggregate. This is significant because it implies that statistically the diabatic terms do not play a major role in determining when the domain aggregates or disaggregates. We expect that while the contribution from diabatic terms may be nonzero for individual cycles, when averaging over multiple cycles, they do not have a specific influence on how the existing state of aggregation will change. This is potentially important for understanding how the frequency of aggregation–disaggregation cycles might change in the real world with climate change and suggests that understanding the change in advective feedbacks will be more important to understand this aspect of aggregation.

We can further observe that vertical advection (Figs. 4a–d) and radiation flux variance terms (Figs. 4i–l) become more positive when the domain is more aggregated. This implies that when the domain is anomalously more aggregated, variance from radiative fluxes and vertical advection is anomalously positive; that is, they act as anomalously positive feedbacks on MSE anomalies. This will tend to sustain the existing anomalous aggregation in the domain. On the other hand, surface fluxes (Figs. 4m–p) and horizontal advection variance terms (Figs. 4e–h)

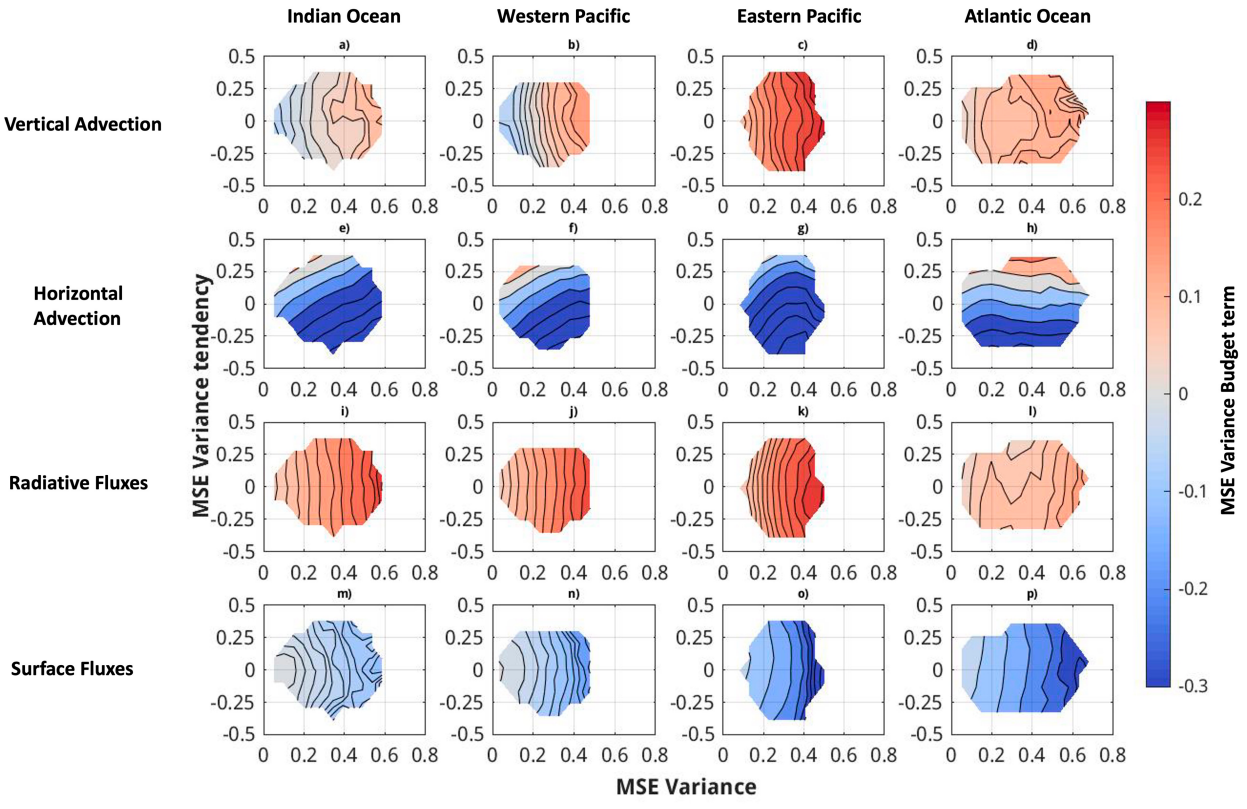

FIG. 4. Bin mean contours of the different MSE variance budget terms from Eq. (2) showing how their value varies across the variance phase space. Columns are the four ocean basins. Rows are the different MSE variance budget terms. (a)–(d) Variance from vertical advection, (e)–(h) variance from horizontal advection, (i)–(l) variance from radiative fluxes, and (m)–(p) variance from surface fluxes. The axes and variance budget term contours are all unitless due to normalization.

become more negative as the domain becomes more aggregated. Therefore, with anomalous aggregation, variance from surface fluxes and horizontal advection is anomalously negative, and they act as anomalously negative feedbacks on MSE anomalies and will tend to dampen the existing anomalous aggregation in the domain.

c. *Contributions to the variability about the mean state–quantitative assessment*

These nuanced relationships between the variability in variance budget terms, MSE variance, and MSE variance tendency can be quantified by computing covariance-based metrics defined by the following equations:

$$M_x = \frac{\overline{\{X\}_a \times \{\langle h\rangle'^2\}_a}}{\overline{\{\langle h\rangle'^2\}_a^2}}, \tag{3}$$

$$E_x = \frac{\overline{\{X\}_a \times \left\{\frac{\partial\langle h\rangle'^2}{\partial t}\right\}_a}}{\overline{\left\{\frac{\partial\langle h\rangle'^2}{\partial t}\right\}_a^2}}. \tag{4}$$

In Eqs. (3) and (4), X represents a term from the MSE variance budget [Eq. (2)], $\{\ldots\}$ represents the domain mean, subscript a represents the time anomaly, and $\overline{X}$ represents the mean of the underlying term across the full time series. The numerator is the covariance between the variance budget term and MSE variance [Eq. (3)] and MSE variance tendency [Eq. (4)]. The covariance is further normalized by the variance of MSE variance and variance of MSE variance tendency. Therefore, the metrics M_x and E_x mathematically represent what ratio of the variance in MSE variance and MSE variance tendency, respectively, can be associated with the particular budget term X. A schematic showing the workflow for the calculation of Eqs. (3) and (4) is shown in Fig. 5.

This method of computing the covariance is analogous to the maintenance and propagation terms calculated in Andersen and Kuang (2012) for the MSE budget. Equation (3) is analog for the maintenance term, and Eq. (4) is analog for the propagation term. Andersen and Kuang (2012) used the word propagation since the changing value of MSE tendency could be associated with the changing phase of the dynamical wave feature as it propagates in space. In the case here, MSE variance tendency does not specifically relate to a spatially propagating feature in the domain. Rather, it simply relates to the evolution of overall aggregation in the domain. Therefore, we will call E_x as the evolution term instead and continue calling M_x as the maintenance term.

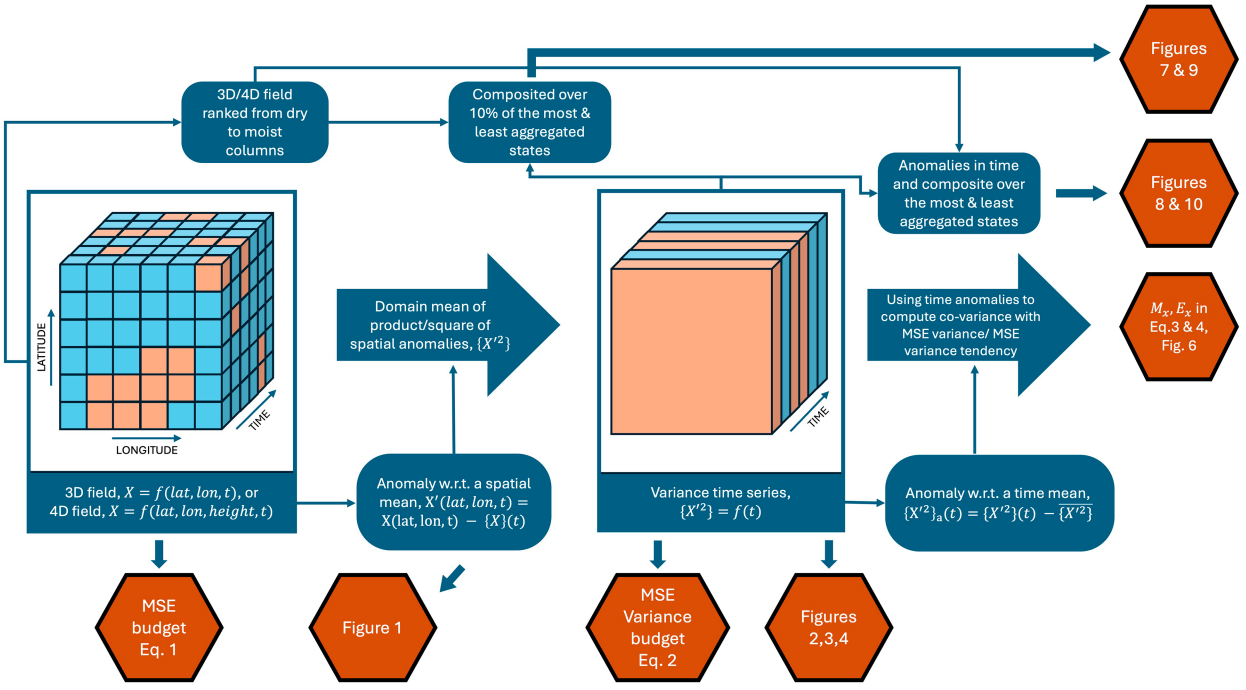

FIG. 5. Schematic showing the data processing workflow for the different metrics and figures being shown in this study.

The maintenance term M_x and evolution term E_x can be interpreted physically in multiple ways. Since they represent the covariability of the budget term X with MSE variance and MSE variance tendency, they represent the role of the term in determining how much the domain aggregates and when the domain aggregates, respectively. The term M_x can also be interpreted in terms of whether the budget term helps maintain the existing aggregation anomaly or not. A positive value implies that the anomalies in X sustain the existing MSE variance anomaly because they have the same sign. A negative value instead indicates that anomalies are of different signs and the budget term has a dampening effect on the existing state. Similarly, E_x can be interpreted as whether the budget term anomalies help sustain or dampen the existing MSE variance tendency.

It should be noted that the notion of the maintenance term here is different from when previous studies have used the term maintenance. While maintenance in this study primarily refers to the maintenance of aggregation anomalies during the aggregation–disaggregation cycle, previous studies used the term in regard to whether a process helps maintain a mean aggregated state. In other words, maintenance in previous studies is related to the mean value of the MSE variance budget term (Fig. 3). In the rest of this paper, by maintenance of aggregation, we will refer to maintenance in the context of aggregation–disaggregation cycles and whether a process is maintaining an aggregation anomaly in the reanalysis. Since this metric measures how the budget term is changing with aggregation anomalies, it also represents how it feeds back onto aggregation. However, to avoid any confusion about the context in which the term feedback is being used, we will use the term feedback only in the context of MSE anomalies. Feedback on aggregation will be referred to as a positive or negative contribution to the maintenance of aggregation anomalies.

Figure 6 shows the maintenance and evolution terms corresponding to each variance budget term for each ocean basin.

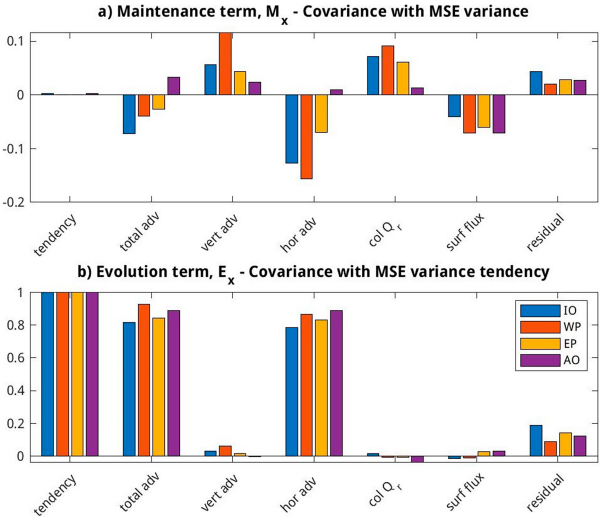

FIG. 6. Bar plot showing the covariance of each MSE variance budget term from Eq. (2) (including residual) to (a) MSE variance–maintenance term computed as per Eq. (3) and (b) MSE variance tendency–evolution term computed as in Eq. (4). Different colors correspond to different ocean basins with IO in blue, WP in orange, EP in yellow, and AO in purple. Evolution term is unitless, and the maintenance term has units of per second.

Figure 6a shows that vertical advection and column radiation fluxes have a positive contribution to maintenance, while horizontal advection and surface fluxes have a negative contribution to the maintenance of aggregation anomalies. This is consistent with Fig. 4 which showed that variability in vertical advection and radiative fluxes helps sustain the existing anomalous aggregated state of the system, and variability in horizontal advection and surface fluxes tends to dampen the existing aggregation anomaly. Similarly, the evolution term in Fig. 6b shows that only variability in horizontal advection covaries positively with MSE variance tendency and is the major factor in understanding when the domain aggregates. These results are fairly insensitive to domain size as long as the domain is large enough and placed appropriately so as to sample both the moist and dry regions.

While these characteristics are qualitatively similar across the different basins, there are also some stark quantitative differences. For example, vertical advection and column radiation have the same sign of impact on maintenance in all ocean basins—a positive contribution—but these terms show larger basin-to-basin variations in magnitude. Contribution from horizontal advection changes even more extremely, showing a flip in sign for the Atlantic basin compared to other domains. These differences can be associated with changes in the contour shapes between the different ocean basins observed in Fig. 4. For example, horizontal advection variance contours in the eastern Pacific and Atlantic Ocean boxes (Figs. 4g,h) are more horizontal as compared to the Indian Ocean or western Pacific boxes (Figs. 4e,f) making their contribution to the maintenance term smaller in magnitude comparatively. This suggests that changes in the magnitude of the contribution to maintenance by the horizontal advection variance term are related to subtle differences in the phase relationship between horizontal advection variance and domain MSE variance rather than an outright difference like a change in sign of the feedback. Similarly, differences in contribution to maintenance from vertical advection variance and radiative flux variance can also be associated with such subtle phase relationships. This implies that, while the maintenance and evolution metrics do a good job of quantifying the nuanced relationships between the variability in variance budget terms and variability in MSE variance/MSE variance tendency, these metrics should be interpreted carefully.

d. Changes in circulation between the most and least aggregated states

A more detailed mechanistic understanding of the processes associated with the variability in aggregation can be developed by connecting changes in variance budget terms with changes in the underlying MSE budget term [Eq. (1)]. For example, consider a positive maintenance term which implies that the variance budget term varies such that it supports an existing aggregation anomaly. Physically, this can happen through multiple pathways depending on whether the particular variance budget term itself is positive or negative, that is, whether it acts as a positive or negative feedback on MSE anomalies in the domain. If it is a positive feedback, then the positive feedback must get stronger with more aggregation to have a positive maintenance term; that is, the process either tends to moisten the moist columns more strongly or dry the dry columns more strongly as the domain becomes more aggregated. In the opposite manner, for a negative variance budget term with a positive contribution to maintenance, the process will either tend to dry the moist columns less strongly or moisten the dry columns less strongly as the domain gets more aggregated.

In this study, we will look at changes in horizontal and vertical advection in greater detail to understand where the observed pattern in the variance term is coming from. We particularly highlight characteristics that can explain the change in variance budget terms and are similar across different regions in the tropics since those must correspond to the more dominant mechanisms. To do so, we look at two things. First, we examine how does column-integrated MSE advection in the moist and dry columns change as the overall domain becomes less or more aggregated. This tells us about the maintenance of aggregation anomalies. Second, we examine how the three-dimensional circulation in the domain boxes changes when the basins are most aggregated compared to when the basins are least aggregated. In Figs. 7–10, column-integrated MSE advection terms and the three-dimensional circulation profiles are plotted as a function of binned column MSE. For each time step, we arrange all grid points in the domain in increasing order of column MSE and then bin them into 10 equal percentile bins to rank high MSE (which we will refer to as moist) and low MSE (dry) columns. The MSE deciles are further composited over 10% of the times when the domain is most and least aggregated to show the differences as the overall domain becomes more or less aggregated. The data processing workflow is summarized in Fig. 5.

1) Horizontal advection and horizontal circulation changes

Figure 7 shows the bin mean horizontal advection of MSE [Eq. (1)] for the column MSE percentile bins in all four domains, composited for when the domain is most aggregated and when it is least aggregated. We observe that horizontal advection is mostly negative (i.e., it has a tendency to reduce MSE in the column) across all the columns in the different regions. However, how the values change with aggregation can differ in different columns and different basins. The moist columns in all four regions show a tendency for horizontal advection to become more negative; i.e., the anomalously moist columns tend to lose more MSE due to horizontal MSE advection with stronger aggregation. In terms of the variance budget, this would imply that changes over the moist columns tend to make the horizontal advection variance term more negative as the domain aggregates. This is a negative contribution to the maintenance of aggregation since it contributes to decreasing the variance more strongly when more aggregated (making a negative feedback more negative). In contrast, horizontal MSE advection tends to export less MSE out of the dry columns in the Indian Ocean and western Pacific basins, while the dry columns show a tendency for stronger MSE advection out of the column in the eastern Pacific and Atlantic Ocean basins as the domains aggregate. Reduced tendency to make the dry columns drier with aggregation is

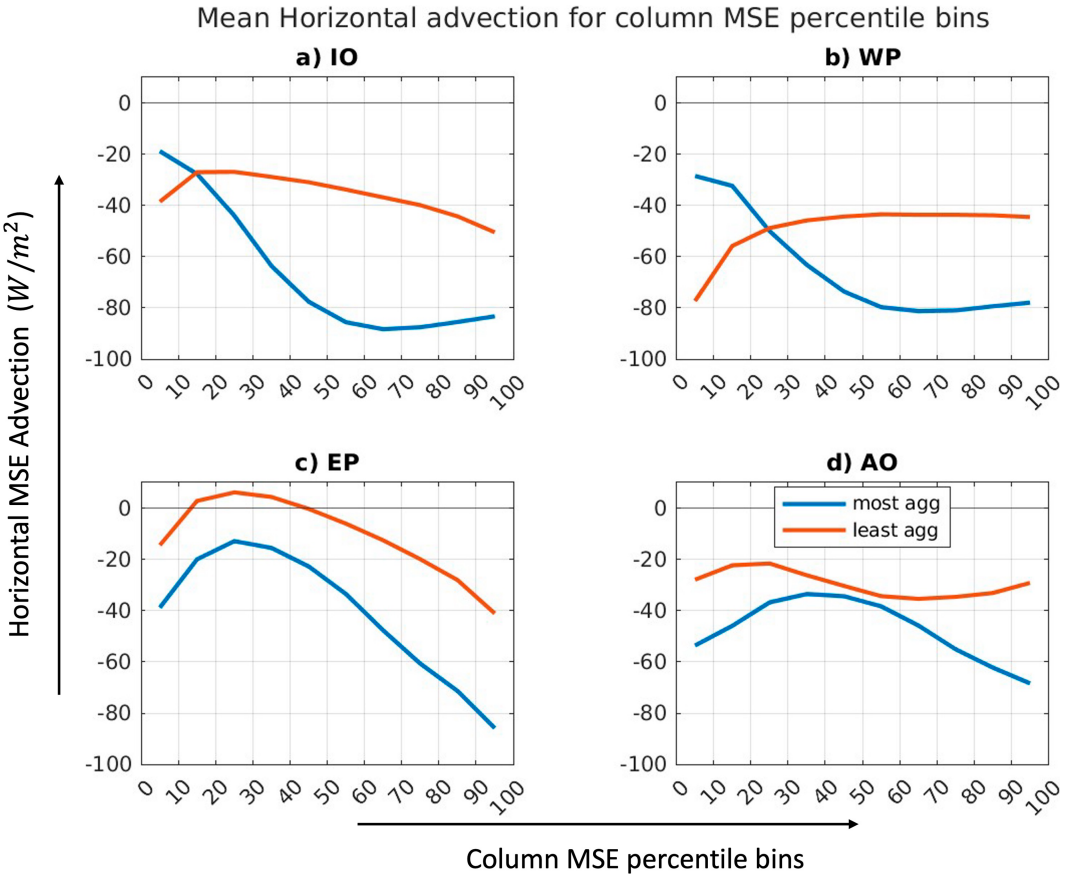

FIG. 7. Bin mean column-integrated horizontal MSE advection for deciles of column MSE in all four ocean boxes when the domain is most aggregated (blue) and when it is least aggregated (red). The x axis represents the deciles of column MSE arranged to go from dry to moist columns as you go left to right.

also a negative maintenance contribution since it implies increased anomalous moistening of the dry columns (making the negative feedback more negative). However, the tendency to make the dry columns drier with aggregation is a positive maintenance contribution. Therefore, we will expect the maintenance term for horizontal advection to be more negative for the Indian Ocean and western Pacific boxes. This is consistent with the observed differences in the magnitude of the maintenance term for horizontal advection in Fig. 6a. It should also be noted that horizontal advection over moist columns changes uniformly with aggregation throughout the different basins, while the dry regions behave differently over different ocean basins.

Next, we will look at the changes in the horizontal circulation during the most and least aggregated states as a function of the binned column MSE bins (Fig. 8). Binning by column MSE distorts the geography of the domain. Therefore, horizontal circulation has to be visualized as flow between dry and moist columns. This is calculated by computing the projection (dot product) of the horizontal wind vector at each grid point along the direction of the MSE gradient. Plotting the bin mean of the projected winds then represents the horizontal winds in the direction of the more moist columns for each bin. To highlight the changes in the horizontal circulation with changing magnitude of aggregation in time, we further compute the time anomaly of the bin mean projected winds before plotting their composites over the most and least aggregated states.

Looking at Figs. 8a and 8b, we observe that when the domain is least aggregated [panel (b)], the anomalous horizontal flow is negative near the surface, meaning that anomalous flow is from moist to dry columns. Conversely, when the domain is more aggregated, the anomalous horizontal flow is from the dry to moist columns near the surface. This indicates that the extent of aggregation in the domain is linked to a reversal in the direction of anomalous horizontal winds. Similar wind change patterns are observed over the other boxes as well (not shown). A recent study by Adames Corraliza and Mayta (2024) has hypothesized that such a change in wind direction could be related to interactions between moisture gradient-driven large-scale organized convection and circulation in the tropics, and this is discussed more in section 4.

2) VERTICAL ADVECTION AND VERTICAL VELOCITY PROFILE CHANGES

Variance due to the vertical advection was found to contribute positively to the maintenance of aggregation anomalies in Fig. 6.

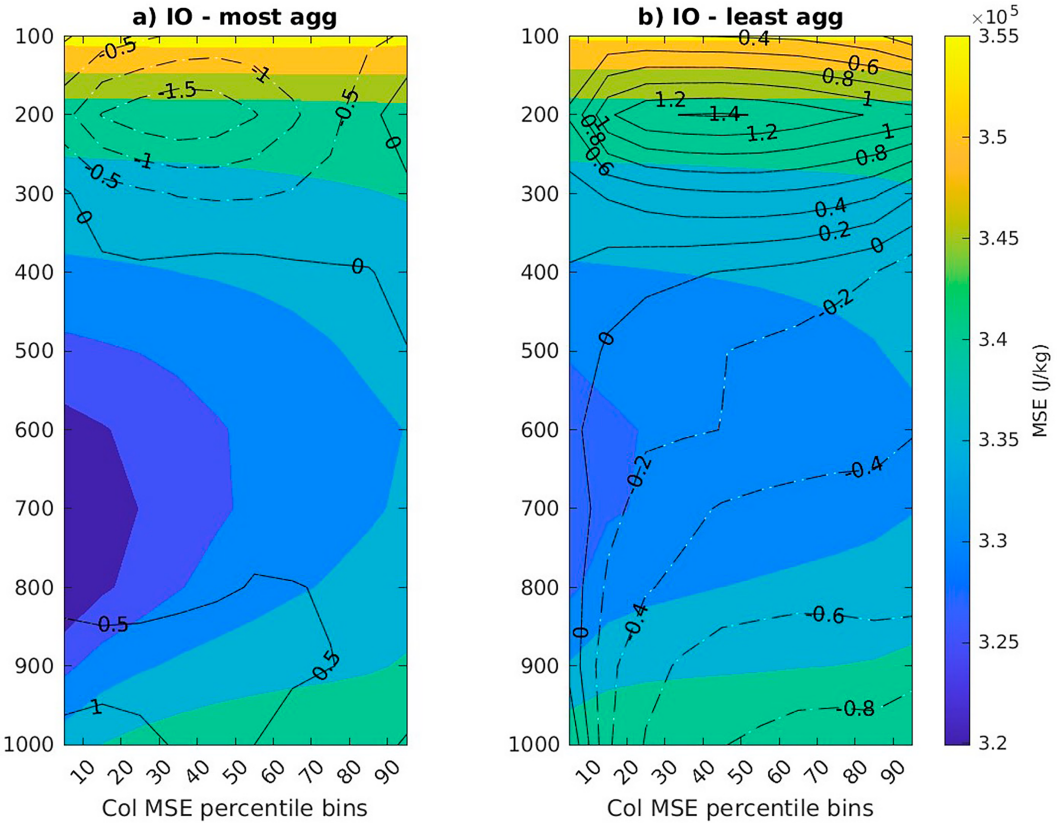

FIG. 8. Contours showing time anomalies of the horizontal winds projected on MSE gradient for IO box composited over (a) 10% of the times when the domain is most aggregated and (b) 10% of the times when the domain is least aggregated. The *y* axis is height in pressure units, and the *x* axis is the deciles of column MSE. Anomalies are computed with respect to a time mean climatological state for each grid point. The contours have units of meters per second. Solid contours mean positive values, and dashed contours mean negative values. For a given column, positive contour values denote that flow is toward moister columns (to the right) and vice versa. Shading represents the vertical MSE profile for the column bins.

Figures 4a–d show that this happens because as the domain becomes more aggregated, variance tendencies from vertical advection become more positive. In theory, this could be attributed to an increased anomalous moistening tendency of the moist columns or an increased anomalous drying tendency of the dry columns due to vertical advection. Further, these changes can be due to a combination of 1) changes in the amount of vertical motion and/or 2) changes in the top heaviness of the vertical motion profile and/or 3) changes in thermodynamic profiles affecting vertical advection without changes in the vertical motion. We wish to diagnose which of these changes is occurring.

Previous idealized modeling studies have highlighted the important role of increased low-level subsidence in dry regions being an important positive feedback for MSE anomalies (Muller and Held 2012). In contrast, Tsai and Mapes (2022) show that ascending vertical motion profiles in the moist columns tend to be more bottom heavy for more aggregated cases over the Indian Ocean in MERRA-2 data. However, other previous studies also discuss how geographic variability in vertical motion profile shape implies geographical differences in how convection amplifies during such cyclical modes (Inoue et al. 2021). This then raises the question: Are there specific patterns in the vertical motion profile shape changes which can be observed consistently across the different ocean basins that can explain the positive contribution of vertical advection variance to maintenance of aggregation in this framework? Are these changes in variance driven by vertical motion profile changes in the dry regions or the moist regions?

Column-integrated vertical MSE advection as a function of binned column MSE and composited over 10% of the most and least aggregated cases for all four domains is shown in Figs. 9a(1)–d(1). Starting off with the Indian Ocean box [Fig. 9a(1)], we observe that the moist columns tend to lose MSE and the dry columns tend to gain MSE due to vertical advection when the domain is less aggregated (orange line). This is representative of vertical advection acting as negative feedback on MSE anomalies when the domain is less aggregated, consistent with Fig. 4a. Further, we observe that the moist columns tend to be dried more by vertical advection as the domain becomes more aggregated (blue line). This is a negative contribution to maintenance as this tends to make a negative variance budget term more negative with anomalous

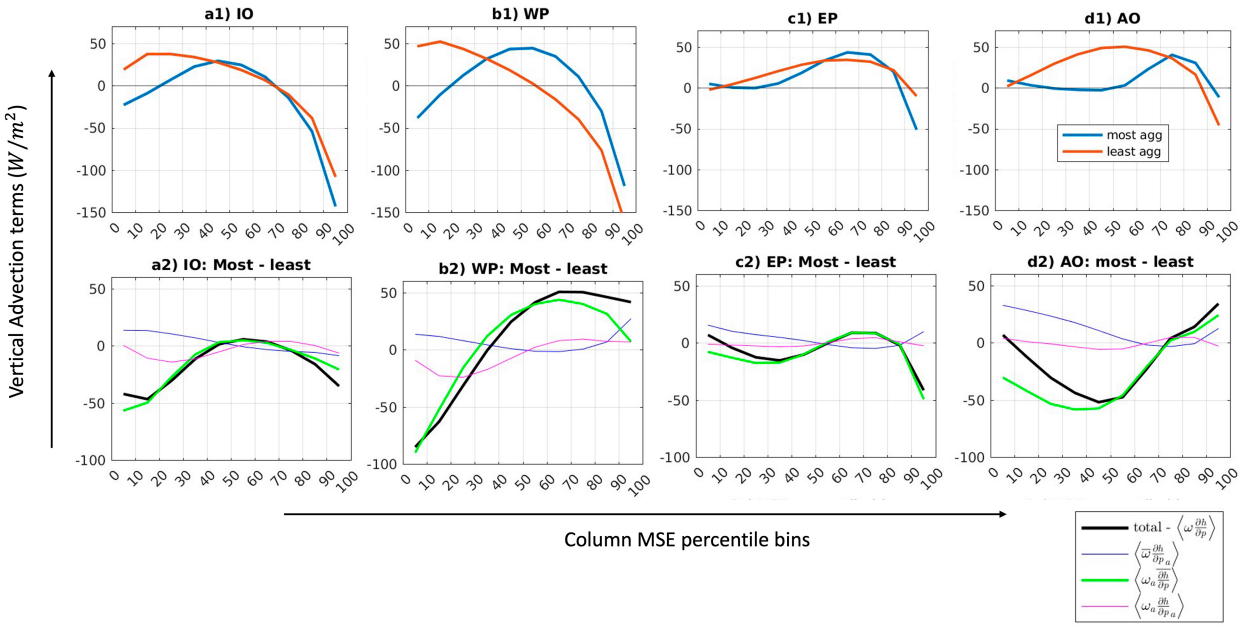

FIG. 9. Bin mean column-integrated vertical advection for deciles of column MSE when the domain is most aggregated (blue) and when it is least aggregated (red) for [a(1)] IO, [b(1)] WP, [c(1)] EP, and [d(1)] AO domains. [a(2)],[b(2)],[c(2)],[d(2)] Black curve represents the differences in total column vertical advection for a given column MSE bin between the most and least aggregated cases for each basin. Other colors represent the differences for various terms in vertical advection decomposition as per Eq. (5).

aggregation. However, dry columns tend to be moistened less by vertical advection at the same time, which is a positive contribution to the maintenance term. Since the total maintenance term for vertical advection variance is positive in the Indian Ocean box as per Fig. 6a, vertical advection changes in the dry columns must dominate over the changes in moist columns.

This change in vertical advection as the domain becomes more aggregated can also be visualized by plotting the difference between the two lines in Fig. 9a(1). This difference is plotted in Fig. 9a(2) in black, which shows the least aggregated case subtracted from the most aggregated case. Negative values denote anomalous drying tendency of the column as domain aggregates, and positive values denote anomalous moistening tendency. Comparing figures for the Indian Ocean box with the other domains (Figs. 9b–d), we observe that while the shape of the vertical advection curve itself can be different between the different domains, all domains show an anomalous drying or a weakened moistening tendency over the dry columns with aggregation due to changes in vertical advection. We also observe that moist columns in the Indian Ocean and eastern Pacific boxes show a stronger anomalous drying tendency as vertical advection changes with aggregation. However, for the western Pacific and Atlantic Ocean boxes, the moist columns show an increased anomalous moistening tendency in the moist columns with aggregation due to vertical advection. This discrepancy suggests that vertical advection changes in the dry or subsiding columns are more uniform across the different regions. Moreover, since vertical advection overall contributes positively to the maintenance of aggregation in all ocean basins (Fig. 6a), these changes over dry columns can be very important to understanding the physical response.

To better understand whether these changes in vertical advection come from changes in the vertical motion profile or from changes in the MSE profile, we decompose vertical advection within each bin as follows:

$$\left\langle \omega \frac{\partial h}{\partial p} \right\rangle = \left\langle \overline{\omega} \frac{\partial \overline{h}}{\partial p} \right\rangle + \left\langle \overline{\omega} \frac{\partial h}{\partial p_a} \right\rangle + \left\langle \omega_a \frac{\partial \overline{h}}{\partial p} \right\rangle + \left\langle \omega_a \frac{\partial h}{\partial p_a} \right\rangle. \tag{5}$$

In this equation, the overbar denotes a time average across the most and least aggregated times and the subscript "a" represents an anomaly from the time mean. The difference between the most and least aggregated states for the decomposed terms is plotted as colored thin lines in Figs. 9a(2)–d(2). Since the mean profiles are constant between the most and least aggregated states, the line corresponding to $\langle \overline{\omega}(\overline{\partial h/\partial p}) \rangle$ will be zero (not shown). We observe that change in total vertical advection is very closely followed by change in $\langle \omega_a(\overline{\partial h/\partial p}) \rangle$, which corresponds to anomalous changes in vertical motion profiles acting on a time mean MSE gradient profile (green). This suggests that variability in vertical advection is mainly explained by the changes in vertical motion profiles between most and least aggregated states. This is observed robustly over all four ocean domains.

Figure 10a shows the vertical profiles of mean vertical velocity (contour) and mean MSE (shading) in the leftmost panel and the time anomalous vertical velocity (contour) and time anomalous MSE (shading) during the most and least aggregated cases in the other two panels for the Indian Ocean domain. As expected, we observe that the mean vertical velocity is ascending over the moist columns and descending over the dry columns. We further observe that the negative MSE anomalies over the drier columns dominate the MSE profile changes as shown by

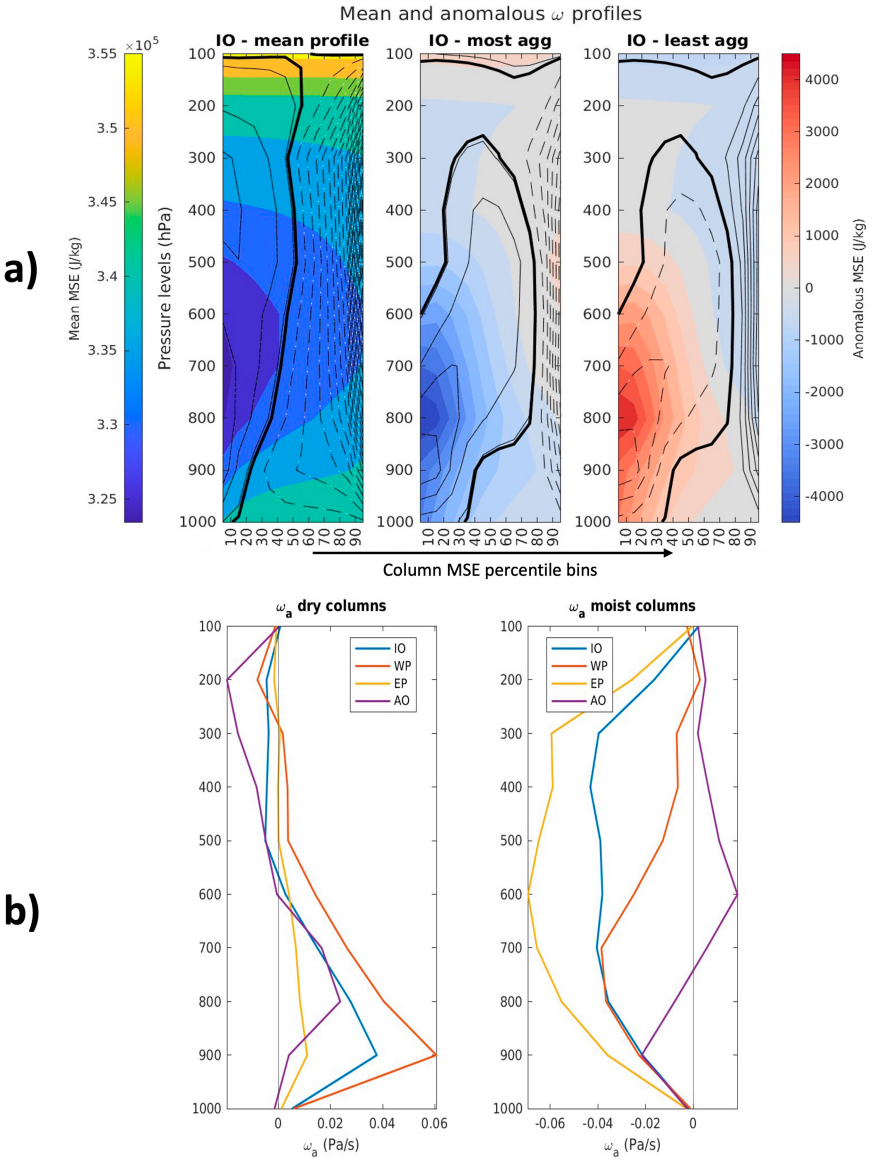

FIG. 10. (a) Mean and anomalous vertical velocity in pascals per second (contours) and MSE in joules per kilogram (shading) for the different column MSE deciles in the IO domain. Mean and anomalies are consistent with definitions for Eq. (5). Panels showing composite over the most and least aggregated cases show anomalies with respect to the mean profiles. Vertical velocity is in pressure coordinates so positive values mean descent and negative values mean ascent. Thick black contour corresponds to the zero contour in all panels. Solid contours represent positive values. Dashed contours represent negative values. Contour levels are spaced every 0.01 Pa s^{-1} for the mean profile and every 0.005 Pa s^{-1} for the anomalous profiles. (b) Anomalous vertical velocity profiles in all four ocean basins over the (left) two driest deciles and (right) two moistest deciles. The anomaly is calculated as the difference between the most and least aggregated composites here.

the range of color shading when the domain is most aggregated. The MSE increase in the moist columns is comparatively closer to zero. In terms of vertical velocity changes, we observe a strong increase in upward vertical velocity over the moist columns with stronger aggregation in the domain. We also observe a stronger low-level subsidence over the dry regions consistent with previous idealized modeling studies. This increase in subsidence combined with the positive vertical MSE gradient at low levels contributes to anomalous negative advection or anomalous drying of the dry columns. This anomalous drying causes the weakening in the moistening tendency over the dry columns discussed above. In contrast, it is not easy to make out if the enhancement of upward vertical velocity over the moistest columns is bottom or top heavy.

Vertical velocity profile changes are better visualized in Fig. 10b which shows the anomalous vertical motion profile for the two driest and two moistest bins from panel (a). The anomalous vertical velocity plotted here is the difference between the most and least aggregated composites. Profiles from all four ocean basins are plotted for easy comparison. Figure 10b clearly shows a ubiquitous increase in low-level subsidence in the dry columns in all ocean basins with aggregation. In contrast, changes over the moistest columns are not uniform. We observe that enhancement of upward motion has a relatively more bottom-heavy profile in the western Pacific and Atlantic Ocean as compared to the Indian Ocean and eastern Pacific. Bottom-heavy ascent can be associated with decreased drying tendency due to vertical advection in the moist columns in the western Pacific and Atlantic Ocean, whereas the relatively more top-heavy ascent strengthens the vertical advective drying tendency of the moist columns in the Indian Ocean and eastern Pacific basins. These differences in the moist regions are consistent with changes observed in Fig. 9.

Idealized modeling studies can disagree on what causes the increase in low-level subsidence in dry regions. Muller and Held (2012) found this to be driven by enhanced low-level radiative cooling in dry regions, whereas Holloway and Woolnough (2016) found the low-level circulation to not be driven by radiative changes in their simulation. Understanding the exact relationship between vertical radiative cooling profiles and their impact on circulation and organization of convection is an open area of current research. Our results support that such feedbacks are important for understanding the maintenance of large-scale aggregation anomalies.

4. Summary and discussion

This study aims to establish a process-oriented framework to visualize and understand the aggregation of convection in the real world through the lens of reanalysis data. To do so, we utilized the spatial variance of MSE over ocean-wide large domains as our metric of aggregation. Defining aggregation based on the spatial variance of MSE allows us to focus on aggregation in terms of its impact on the large-scale environment, providing a different perspective to the one obtained from studying aggregation through the characterization of cloud organization at smaller scales. Also, the domain sizes in this study are much bigger than the $10^\circ \times 10^\circ$ boxes used in previous work (Tobin et al. 2012; Tompkins and Semie 2017; Masunaga et al. 2021, etc.). This shifts the focus from aggregation at mesoscales to aggregation at larger scales in this study. The results presented in this study are fairly insensitive to minor changes ($<5^\circ$) in domain size and placement. For larger variations in domain size, the overall results are found to be qualitatively similar as long as the domain is large enough to sample both the moist and dry regions associated with large-scale aggregation adequately (not shown).

We develop a new phase space to visualize the evolution of aggregation in the form of the MSE variance phase space. This framework puts domain MSE variance on the x axis (extent of aggregation) and the tendency of MSE variance on the y axis (changes in aggregation). We highlight the distinction between the mean aggregated state and the variability about the mean state. A composite vector plot showing the evolution of aggregation on the phase space highlights the cyclical mode of variability in aggregation about the mean state. We call these the aggregation–disaggregation cycles (Fig. 2). While previous studies have mostly focused on characteristics of the mean aggregated state, this study focuses on characterizing the variability about the mean state which may be observed in some models but has not been explored systematically. This visualization, by construction, puts the emphasis on this mode of variability as a key feature of aggregation in the real world. This is complementary to the major theme of most self-aggregation studies, which tend to highlight the characteristics of the quasi-equilibrium mean state as the key feature of aggregation.

Different terms of the MSE variance budget [Eq. (2)] represent the different processes that can contribute to aggregation or disaggregation, impacting both the mean state and the observed variability. The different terms include variance from vertical advection, horizontal advection, radiative fluxes, and surface fluxes. To characterize the evolution of variability in aggregation, we focus on two aspects: first, how much the domain aggregates, and second, when the domain aggregates. This is evaluated with the help of the maintenance [Eq. (3)] and evolution [Eq. (4)] metrics defined in this study. The maintenance term is related to how much the domain aggregates, and the evolution term is related to when the domain aggregates. This is different from previous notions of maintenance of aggregation which focus more on the maintenance of the mean aggregated state, while here we focus on the maintenance of aggregation anomalies about the mean state. This is also summarized with the help of a schematic in Fig. 11.

Key features observed throughout different regions in the tropics are listed below:

- For the mean state (Fig. 3), we find surface fluxes and horizontal advection tend to resist aggregation, while radiative fluxes tend to support aggregation throughout the tropics. Further, vertical advection does not tend to resist aggregation. It either tends to support aggregation or has close to zero impact on the mean aggregated state in the different basins. Contributions to the mean state are broadly consistent with previous idealized modeling studies.
- Our results highlight that only the variance from horizontal advection plays a role in determining when the domain aggregates and disaggregates (Fig. 6b). Hence, horizontal advection acts as a driver for aggregation–disaggregation cycles. All four budget terms have a significant role in contributing to the strength of aggregation anomalies or how much the domain aggregates.

Contribution to the strength of aggregation anomalies is related to how the budget term feeds back onto aggregation. We find that surface fluxes and horizontal advection tend to dampen aggregation anomalies more strongly when the domain is more aggregated, while radiative fluxes and vertical advection tend to amplify aggregation anomalies more strongly (Fig. 6a). We explore the advective feedbacks in greater detail in this study. However, based on previous

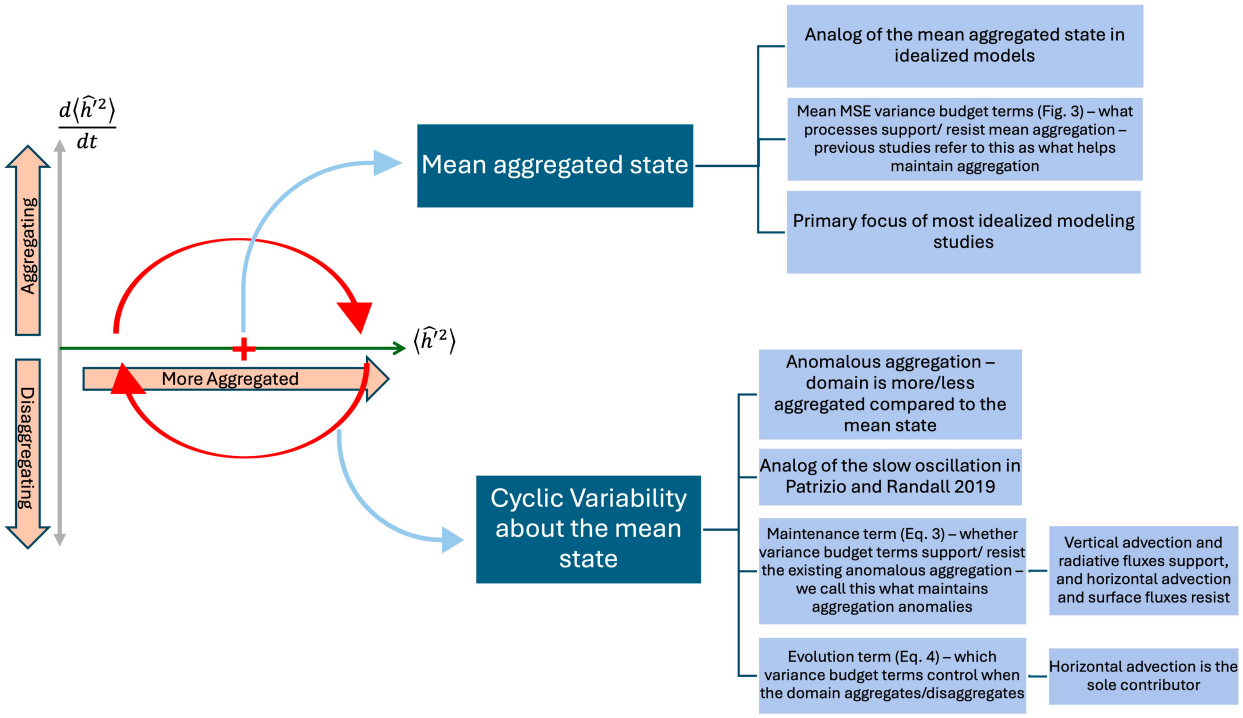

FIG. 11. Schematic summarizing the mean aggregated state versus the variability about the mean state behavior of aggregation in the observed world being discussed in this study.

studies, we expect increased air–sea enthalpy disequilibrium over the dry regions during a more aggregated state to drive stronger moistening tendencies by surface fluxes which will tend to dampen the aggregation anomaly (Wing and Emanuel 2014; Pope et al. 2023). For radiative fluxes, we expect increased high clouds and water vapor in the moist regions to drive increased moistening which will tend to amplify the aggregation anomaly (Pope et al. 2021, 2023).

We show that vertical advection broadly tends to moisten the dry columns in the domain. However, as the domain becomes more aggregated, we observe that vertical advection tends to moisten the dry columns less as compared to the least aggregated states (Fig. 9). This tends to support the existing aggregation anomalies in the domain. While the change in vertical advection over the dry columns is qualitatively consistent over all ocean basins, changes over the moist columns can differ between the different regions. Looking at the vertical velocity profiles reveals that the low-level subsidence over the drier columns is enhanced across all ocean basins when the domain is more aggregated which supports the weakening tendency to moisten the drier columns (Fig. 10). Moist columns instead show differences in top heaviness of the enhanced ascending profiles in different basins which can explain why changes in vertical advection are not consistent for the moist columns over different basins in Fig. 9. Since the changes in vertical advection over the dry columns are consistent across the domains, and their effect on supporting existing aggregation anomalies in the domain is qualitatively consistent with the effect of the overall vertical advection variance term, we expect the response in dry columns to be the more dominant mechanism.

Similarly, we observe that horizontal advection tends to dry the moist columns more strongly as the domain becomes more aggregated in all ocean basins (Fig. 7). In contrast, changes in horizontal advection over the dry columns are not consistent across the ocean basins. However, the increased drying tendencies over the moist columns in more aggregated states are larger in magnitude and explain the increased tendency to damp the aggregation anomalies by horizontal advection. The three-dimensional structure of the horizontal circulation shows that anomalous horizontal circulation changes in direction with aggregation. The anomalous horizontal flow is from the dry to moist columns in lower levels when the domain is more aggregated and is from moist to dry columns when the domain is less aggregated.

Observation about the change in horizontal wind direction in this study is also consistent with recent studies presenting observational and theoretical evidence for horizontal moisture gradient-driven moisture modes (Mayta and Adames Corraliza 2024; Adames Corraliza and Mayta 2024). Similar to aggregation–disaggregation cycles, these moisture modes were also found to be driven by horizontal advection. As per this theory, the presence of strong moisture gradients in the domain spins up moisture mode eddies which act to even out the moisture mode gradient (Adames Corraliza and Mayta 2024). Therefore, the existence of strong eddy flow from moist to dry columns should lead to small moisture gradients and a less aggregated domain, while the absence of eddy flow should lead to the buildup of strong moisture gradients and a

more aggregated state. This could be a possible hypothesis for how horizontal advection can drive the propagation of the aggregation–disaggregation cycles and explain the structure of horizontal circulation we observe in our results. If true, this suggests that the large-scale aggregation being observed here can be thought of in terms of a strong ITCZ or Hadley cell circulation. The moisture modes, which manifest at smaller scales, then act as a disaggregation process. This could be a significant change in how we think about aggregation manifesting in the real world. Moisture modes, which traditionally were thought to be an example of aggregation at synoptic scales, could also be contributing to disaggregation at larger planetary scales. This also highlights the multiscale nature of aggregation and the importance of understanding the cross-scale interactions if we wish to understand the full picture of how aggregation evolves in the real world.

Another interesting aspect of these results is the similarities and differences with the expectations based on idealized model studies. Our results show that while radiative fluxes are important for the maintenance of aggregation–disaggregation cycles, that does not mean that they control when the domain will aggregate or disaggregate. Rather, that is governed by horizontal advection. Therefore, understanding horizontal advection and how that may change with climate change will be an important factor in understanding aggregation under a changing climate, particularly the frequency of aggregation. Wing (2019) discusses how the frequency of aggregation is important for its impact on climate and extreme precipitation events in the real world. The aggregation–disaggregation cycles we study in this work are expected to be relevant for understanding the aggregation that is associated with precipitation extremes. Hence, these aggregation–disaggregation cycles are worthy of further study.

Acknowledgments. This work was supported in part by funding from National Science Foundation Award 1759793. Maithel would like to thank Victor Mayta for help with MSE budget calculations from raw ERA5 data. The authors would also like to thank Ángel Adames-Corraliza for helpful discussions that motivated the creation of Fig. 8. The authors thank Brandon Wolding, Brian Mapes, and three anonymous reviewers whose feedbacks have greatly helped improve the quality of this manuscript.

Data availability statement. ERA5 data used in the study are available at https://doi.org/10.24381/cds.bd0915c6.

REFERENCES

Adames, Á. F., and E. D. Maloney, 2021: Moisture mode theory's contribution to advances in our understanding of the Madden-Julian oscillation and other tropical disturbances. *Curr. Climate Change Rep.*, **7**, 72–85, https://doi.org/10.1007/s40641-021-00172-4.

Adames Corraliza, Á. F., and V. C. Mayta, 2024: The stirring tropics: Theory of moisture mode–Hadley cell interactions. *J. Climate*, **37**, 1383–1401, https://doi.org/10.1175/JCLI-D-23-0147.1.

Andersen, J. A., and Z. Kuang, 2012: Moist static energy budget of MJO-like disturbances in the atmosphere of a zonally symmetric aquaplanet. *J. Climate*, **25**, 2782–2804, https://doi.org/10.1175/JCLI-D-11-00168.1.

Arnold, N. P., and D. A. Randall, 2015: Global-scale convective aggregation: Implications for the Madden-Julian Oscillation. *J. Adv. Model. Earth Syst.*, **7**, 1499–1518, https://doi.org/10.1002/2015MS000498.

Back, L. E., and C. S. Bretherton, 2006: Geographic variability in the export of moist static energy and vertical motion profiles in the tropical Pacific. *Geophys. Res. Lett.*, **33**, L17810, https://doi.org/10.1029/2006GL026672.

——, Z. Hansen, and Z. Handlos, 2017: Estimating vertical motion profile top-heaviness: Reanalysis compared to satellite-based observations and stratiform rain fraction. *J. Atmos. Sci.*, **74**, 855–864, https://doi.org/10.1175/JAS-D-16-0062.1.

Becker, T., and A. A. Wing, 2020: Understanding the extreme spread in climate sensitivity within the Radiative-Convective Equilibrium Model Intercomparison Project. *J. Adv. Model. Earth Syst.*, **12**, e2020MS002165, https://doi.org/10.1029/2020MS002165.

Beucler, T., T. H. Abbott, T. W. Cronin, and M. S. Pritchard, 2019: Comparing convective self-aggregation in idealized models to observed moist static energy variability near the equator. *Geophys. Res. Lett.*, **46**, 10 589–10 598, https://doi.org/10.1029/2019GL084130.

——, D. Leutwyler, and J. M. Windmiller, 2020: Quantifying convective aggregation using the tropical moist margin's length. *J. Adv. Model. Earth Syst.*, **12**, e2020MS002092, https://doi.org/10.1029/2020MS002092.

Bony, S., A. Semie, R. J. Kramer, B. Soden, A. M. Tompkins, and K. A. Emanuel, 2020: Observed modulation of the tropical radiation budget by deep convective organization and lower-tropospheric stability. *AGU Adv.*, **1**, e2019AV000155, https://doi.org/10.1029/2019AV000155.

Bretherton, C. S., and M. F. Khairoutdinov, 2015: Convective self-aggregation feedbacks in near-global cloud-resolving simulations of an aquaplanet. *J. Adv. Model. Earth Syst.*, **7**, 1765–1787, https://doi.org/10.1002/2015MS000499.

——, M. E. Peters, and L. E. Back, 2004: Relationships between water vapor path and precipitation over the tropical oceans. *J. Climate*, **17**, 1517–1528, https://doi.org/10.1175/1520-0442(2004)017%3C1517:RBWVPA%3E2.0.CO;2.

——, P. N. Blossey, and M. Khairoutdinov, 2005: An energy-balance analysis of deep convective self-aggregation above uniform SST. *J. Atmos. Sci.*, **62**, 4273–4292, https://doi.org/10.1175/JAS3614.1.

Coppin, D., and S. Bony, 2015: Physical mechanisms controlling the initiation of convective self-aggregation in a General Circulation Model. *J. Adv. Model. Earth Syst.*, **7**, 2060–2078, https://doi.org/10.1002/2015MS000571.

Cronin, T. W., and A. A. Wing, 2017: Clouds, circulation, and climate sensitivity in a radiative-convective equilibrium channel model. *J. Adv. Model. Earth Syst.*, **9**, 2883–2905, https://doi.org/10.1002/2017MS001111.

Dirkes, C. A., A. A. Wing, S. J. Camargo, and D. Kim, 2023: Process-oriented diagnosis of tropical cyclones in reanalyses using a moist static energy variance budget. *J. Climate*, **36**, 5293–5317, https://doi.org/10.1175/JCLI-D-22-0384.1.

Held, I. M., R. S. Hemler, and V. Ramaswamy, 1993: Radiative-convective equilibrium with explicit two-dimensional moist convection. *J. Atmos. Sci.*, **50**, 3909–3927, https://doi.org/10.1175/1520-0469(1993)050%3C3909:RCEWET%3E2.0.CO;2.

Holloway, C. E., and S. J. Woolnough, 2016: The sensitivity of convective aggregation to diabatic processes in idealized radiative-convective equilibrium simulations. *J. Adv. Model. Earth Syst.*, **8**, 166–195, https://doi.org/10.1002/2015MS000511.

——, A. A. Wing, S. Bony, C. Muller, H. Masunaga, T. S. L'Ecuyer, D. D. Turner, and P. Zuidema, 2017: Observing convective aggregation. *Surv. Geophys.*, **38**, 1199–1236, https://doi.org/10.1007/s10712-017-9419-1.

Inoue, K., and L. E. Back, 2017: Gross moist stability analysis: Assessment of satellite-based products in the GMS plane. *J. Atmos. Sci.*, **74**, 1819–1837, https://doi.org/10.1175/JAS-D-16-0218.1.

——, M. Biasutti, and A. M. Fridlind, 2021: Evidence that horizontal moisture advection regulates the ubiquitous amplification of rainfall variability over tropical oceans. *J. Atmos. Sci.*, **78**, 529–547, https://doi.org/10.1175/JAS-D-20-0201.1.

Jakob, C., M. S. Singh, and L. Jungandreas, 2019: Radiative convective equilibrium and organized convection: An observational perspective. *J. Geophys. Res. Atmos.*, **124**, 5418–5430, https://doi.org/10.1029/2018JD030092.

Kadoya, T., and H. Masunaga, 2018: New observational metrics of convective self-aggregation: Methodology and a case study. *J. Meteor. Soc. Japan*, **96**, 535–548, https://doi.org/10.2151/jmsj.2018-054.

Lebsock, M. D., T. S. L'Ecuyer, and R. Pincus, 2017: An observational view of relationships between moisture aggregation, cloud, and radiative heating profiles. *Surv. Geophys.*, **38**, 1237–1254, https://doi.org/10.1007/s10712-017-9443-1.

Maithel, V., and L. Back, 2022: Moisture recharge–discharge cycles: A gross moist stability–based phase angle perspective. *J. Atmos. Sci.*, **79**, 2401–2417, https://doi.org/10.1175/JAS-D-21-0297.1.

Maloney, E. D., 2009: The moist static energy budget of a composite tropical intraseasonal oscillation in a climate model. *J. Climate*, **22**, 711–729, https://doi.org/10.1175/2008JCLI2542.1.

Mapes, B. E., E. S. Chung, W. M. Hannah, H. Masunaga, A. J. Wimmers, and C. S. Velden, 2018: The meandering margin of the meteorological moist tropics. *Geophys. Res. Lett.*, **45**, 1177–1184, https://doi.org/10.1002/2017GL076440.

Masunaga, H., C. E. Holloway, H. Kanamori, S. Bony, and T. H. M. Stein, 2021: Transient aggregation of convection: Observed behavior and underlying processes. *J. Climate*, **34**, 1685–1700, https://doi.org/10.1175/JCLI-D-19-0933.1.

Mayta, V. C., and Á. F. Adames Corraliza, 2024: The stirring tropics: The ubiquity of moisture modes and moisture–vortex instability. *J. Climate*, **37**, 1981–1998, https://doi.org/10.1175/JCLI-D-23-0145.1.

Muller, C. J., and I. M. Held, 2012: Detailed investigation of the self-aggregation of convection in cloud-resolving simulations. *J. Atmos. Sci.*, **69**, 2551–2565, https://doi.org/10.1175/JAS-D-11-0257.1.

Patrizio, C. R., and D. A. Randall, 2019: Sensitivity of convective self-aggregation to domain size. *J. Adv. Model. Earth Syst.*, **11**, 1995–2019, https://doi.org/10.1029/2019MS001672.

Pope, K. N., C. E. Holloway, T. R. Jones, and T. H. M. Stein, 2021: Cloud-radiation interactions and their contributions to convective self-aggregation. *J. Adv. Model. Earth Syst.*, **13**, e2021MS002535, https://doi.org/10.1029/2021MS002535.

——, ——, ——, and ——, 2023: Radiation, clouds, and self-aggregation in RCEMIP simulations. *J. Adv. Model. Earth Syst.*, **15**, e2022MS003317, https://doi.org/10.1029/2022MS003317.

Sakaeda, N., and G. Torri, 2022: The behaviors of intraseasonal cloud organization during DYNAMO/AMIE. *J. Geophys. Res. Atmos.*, **127**, e2021JD035749, https://doi.org/10.1029/2021JD035749.

Silvers, L. G., B. Stevens, T. Mauritsen, and M. Giorgetta, 2016: Radiative convective equilibrium as a framework for studying the interaction between convection and its large-scale environment. *J. Adv. Model. Earth Syst.*, **8**, 1330–1344, https://doi.org/10.1002/2016MS000629.

Sobel, A. H., J. Nilsson, and L. M. Polvani, 2001: The weak temperature gradient approximation and balanced tropical moisture waves. *J. Atmos. Sci.*, **58**, 3650–3665, https://doi.org/10.1175/1520-0469(2001)058%3C3650:TWTGAA%3E2.0.CO;2.

Stein, T. H. M., C. E. Holloway, I. Tobin, and S. Bony, 2017: Observed relationships between cloud vertical structure and convective aggregation over tropical ocean. *J. Climate*, **30**, 2187–2207, https://doi.org/10.1175/JCLI-D-16-0125.1.

Su, H., and J. D. Neelin, 2002: Teleconnection mechanisms for tropical Pacific descent anomalies during El Niño. *J. Atmos. Sci.*, **59**, 2694–2712, https://doi.org/10.1175/1520-0469(2002)059%3C2694:TMFTPD%3E2.0.CO;2.

Tobin, I., S. Bony, and R. Roca, 2012: Observational evidence for relationships between the degree of aggregation of deep convection, water vapor, surface fluxes, and radiation. *J. Climate*, **25**, 6885–6904, https://doi.org/10.1175/JCLI-D-11-00258.1.

Tompkins, A. M., and A. G. Semie, 2017: Organization of tropical convection in low vertical wind shears: Role of updraft entrainment. *J. Adv. Model. Earth Syst.*, **9**, 1046–1068, https://doi.org/10.1002/2016MS000802.

Tsai, W.-M., and B. E. Mapes, 2022: Evidence of aggregation dependence of 5°-scale tropical convective evolution using a gross moist stability framework. *J. Atmos. Sci.*, **79**, 1385–1404, https://doi.org/10.1175/JAS-D-21-0253.1.

Wing, A. A., 2019: Self-aggregation of deep convection and its implications for climate. *Curr. Climate Change Rep.*, **5** (1), 1–11, https://doi.org/10.1007/s40641-019-00120-3.

——, 2022: Acceleration of tropical cyclone development by cloud-radiative feedbacks. *J. Atmos. Sci.*, **79**, 2285–2305, https://doi.org/10.1175/JAS-D-21-0227.1.

——, and K. A. Emanuel, 2014: Physical mechanisms controlling self-aggregation of convection in idealized numerical modeling simulations. *J. Adv. Model. Earth Syst.*, **6**, 59–74, https://doi.org/10.1002/2013MS000269.

——, and T. W. Cronin, 2016: Self-aggregation of convection in long channel geometry. *Quart. J. Roy. Meteor. Soc.*, **142** (694), 1–15, https://doi.org/10.1002/qj.2628.

——, K. Emanuel, C. E. Holloway, and C. Muller, 2017: Convective self-aggregation in numerical simulations: A review. *Surv. Geophys.*, **38**, 1173–1197, https://doi.org/10.1007/s10712-017-9408-4.

——, K. A. Reed, M. Satoh, B. Stevens, S. Bony, and T. Ohno, 2018: Radiative–convective equilibrium model intercomparison project. *Geosci. Model Dev.*, **11**, 793–813, https://doi.org/10.5194/gmd-11-793-2018.

——, and Coauthors, 2019: Moist static energy budget analysis of tropical cyclone intensification in high-resolution climate models. *J. Climate*, **32**, 6071–6095, https://doi.org/10.1175/JCLI-D-18-0599.1.

——, and Coauthors, 2020: Clouds and convective self-aggregation in a multimodel ensemble of radiative-convective equilibrium simulations. *J. Adv. Model. Earth Syst.*, **12**, e2020MS002138, https://doi.org/10.1029/2020MS002138.